Proc. Schl. Eng. Tokai Univ., Ser. E
32 (2007) 13 - 17

Influence of Internal Damping on Vibration and Acoustic Radiation Characteristics of Rectangular Plate

by

Yoshihiro OSAKA[*1], Masahiko MIZUOCHI[*2], and Hiroyuki MORIYAMA[*3]

(Received on Mar. 31, 2007 & accepted on Jul. 4, 2007)

Abstract

In this paper, the effect of internal damping on the vibration and acoustic radiation characteristics of rectangular plates is investigated. Plates are assumed to be constructed of aluminum and to be clamped along the four sides. The characteristics are studied by FEM analysis and an experiment. First of all, the internal-damping characteristics of the aluminum are investigated in an excitation experiment using a beam-shaped test specimen and are evaluated on the basis of the loss coefficient, and it is clarified that the loss coefficient increases slightly with excitation frequency. In particular, a polyolefin film, used for varying the internal-damping characteristics, causes the characteristics to depend more strongly on excitation frequency than those of the test specimen not having the film. In the case of the plate, the natural frequency is hardly affected by internal damping, whereas internal damping induces changes in the vibration mode and the amplitude of flexural displacement. In particular, the vibration mode influences not only the appearance but also the modal shape of the plate. Consequently, the acoustic radiation is affected by changes in the modal shape caused by internal damping from the point of view of the distribution characteristics.

Keywords: Rectangular Plate, Internal Damping, Plate Vibration, Radiation Sound Field

1. Introduction

A radiation sound filed is formed by a structural vibration when periodic forces are applied to a thin structure. It is one of the most important problems in sound environment to control the radiation sound generated by this structural vibration. With respect to such a thin structure, a lot of investigations, in which vibration and acoustic problems were discussed, have already reported. In related investigations, the interesting results, as prediction of the sound radiation power and sound pressure distribution for the radiation sound filed formed by driven plate, were also reported[(1)-(3)]. According to these results, it was clarified that the acoustic radiation efficiency, which enables to estimate quantitatively the radiation sound characteristics of rectangular plate, was affected by internal damping of materials. However, because real internal damping is minute, it is difficult to estimate precisely it in a loss coefficient and so on. Therefore, in these investigations, an analytical model having real internal damping wasn't considered, so that these analytical results weren't verified experimentally.

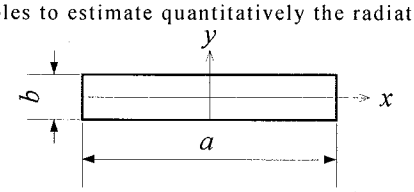

(a) Front view

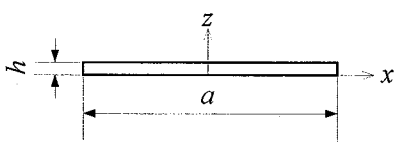

(b) Side view

Fig.1 Beam-shaped test specimen

In the present investigation, the rectangular plate is assumed to be constructed of aluminum and to be clamped along the four sides, so that internal-damping characteristics of the aluminum are investigated in an excitation experiment using a beam-shaped test specimen and are evaluated based on the loss coefficient. When a point force is applied to the plate, vibration and acoustic radiation characteristics are obtained from FEM analysis and experiment. Based on those characteristics, the influence of internal damping is estimated from the point view of distribution characteristics of the flexural displacement and radiation sound field with respect to the plate vibration.

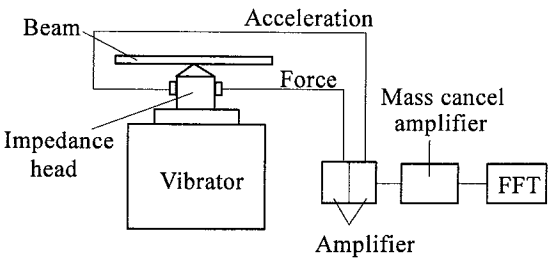

Fig.2 Apparatus to measure loss coefficient

＊1 Graduate Student, Course of Mechanical Engineering
＊2 Nippon Seiki Co., Ltd.
＊3 Professor, Department of Prime Mover Engineering

2. Experimental and analytical models

Figures 1 (a) and (b) show dimensions of the beam-shaped test specimen to measure the loss coefficient of material constructing the rectangular plate, which is the aluminum having Young's modulus E of 71GPa, density ρ of 2680kg/m^3 and Poisson's ratio ν of 0.33. The dimensions have the short side lengths b of 10mm and 14mm and the thicknesses h of 2mm, 3mm and 4mm; the longitudinal length a is set as the aspect ratio a/b is 20,being a principal factor to determine vibration characteristics of the beam. These beams are put on the impedance head, as shown in Fig.2, fixed by an adhesive as the y axis is at the supporting part. In the experiment to obtain the loss coefficient η, the force and acceleration applied to the beam are measured in spectra by the impedance head and FFT analyzer when the beam is excited by a random wave. We adopt the method of half width at half maximum with respect to those spectra, with which loss coefficient η is evaluated.

Figures 3 (a) and (b) show the front and side views of the analytical model used for FEM analysis, respectively. The rectangular plate considered herein has side lengths L_x and L_y of 500mm and 350mm and thicknesses h of 2mm and 4mm. The analytical volume for acoustic radiation is the product of A_x, A_y and A_z that are 500mm, respectively, and is restricted to a quarter region over the x-y plane including the rectangular plate, because the total element number of the analytical model exceeds a limited number if that volume expands into all the region. However, plate vibration modes have to consist of symmetric motion with respect to the x and y axes. On the other hand, the analytical region for plate vibration is all the plate area except for coupling analysis with the acoustic radiation. In this FEM analysis, carried out when the damping coefficient varies, free and forced vibration analyses and acoustic radiation analysis bring natural frequencies, modal shape and vibration power of the plate vibration and acoustic power in the radiation sound field. Here, the vibration mode of the plate is expressed by means of (m,n), combined by numbers of nodes that appear along x and y axes; thus, the natural frequency is expressed by f_{mn}.

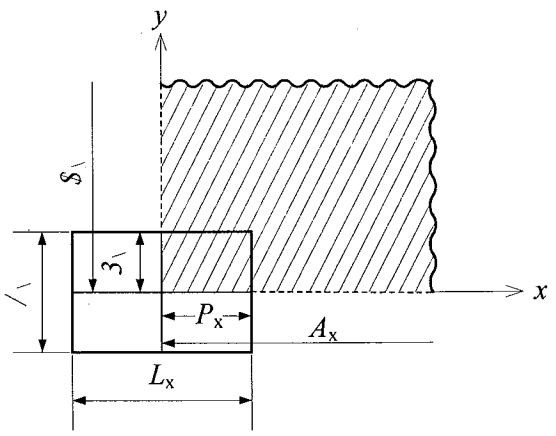

(a) Front view

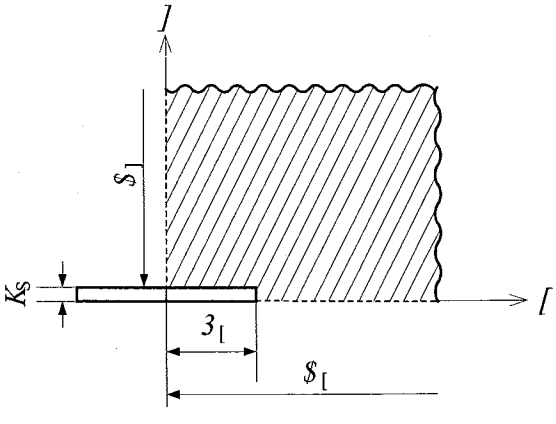

(b) Side view

Fig.3 Experimental and analytical models

In order to verify the result of FEM analysis, obtained from experiments, for which the rectangular plate similar to the analytical model is used, characteristics of the plate vibration and acoustic radiation are compared with those of FEM analysis. The plate is supported by angle members constructed of steel and having each side length of 50mm on the cross section to realize clamped support. Regarded as free vibration characteristics of the plate, the natural frequency and vibration mode are measured using the experimental modal analysis, in which the method moving a point hit with the impulse hammer is adopted. The hitting points to 54 points, which are fixed to the respective x and y directions by intervals of 50mm on the plate.

In the excitation experiment, a point force, whose excitation frequencies are selected from among natural frequencies with reference to free vibration characteristics, is placed at the center of the plate to symmetrize plate motion with respect to the x and y axes. Measured using an accelerometer on the above lattice having 54 points and using a condenser microphone located on z of 50mm over the lattice, the plate vibration and the sound pressure of acoustic radiation caused by the vibration are represented as distributions of the flexural displacement and the sound pressure level, respectively.

The damping characteristics of the rectangular plate need to be varied to make a comparison between the experimental and numerical results, so that a polyolefin film, which is useful for protecting a surface, is used as a film layer on surface of the plate and has E of 650MPa, ρ of 900kg/m^3, ν of 0.3 and h of 50μm. This film is used not only for the above experiment of rectangular plate but also for the experiment to study the damping characteristics.

3. Results and discussion

3.1 Damping characteristics of aluminium

Figure 4 shows the relationship between the loss coefficient η of the aluminum and the natural frequency f_m, which is taken into account until the 5th eigenfrequency of the beam vibration, and the influence of the film on η. The influence is estimated by the difference between η of nonfilmed and filmed beams. In the case of the nonfilmed beam, a small error is included in η, however, it can be confirmed that η increases slightly with f_m that is shifted by changes in thickness and length of the beam. Thus, although η has dependence on f_m, it is possible to regard η as a uniform value in somewhat narrow band with respect to f_m. In the case of the filmed beam, the dependence of η on frequencies becomes clearer, so that the difference between the loss coefficients of the filmed and nonfilmed beams increases, according as the beam vibration comes

to be higher order.

Because damping coefficient β is assumed in this FEM analysis, its damping coefficient β can be expressed by using η as follows:

$$\beta = \frac{\eta}{2\pi f_m} \quad \cdots\cdots\cdots\cdots\cdots\cdots\cdots\cdots (1)$$

Figure 5 indicates β calculated with substituting η in Fig.4 into Eq.(1). η increased with the f_m, whereas β decreases greatly with the increase of f_m up to the proximity of 3000Hz, having the frequency term in the denominator into the expression of Eq.(1). In the frequency range beyond 3000Hz, β of the nonfilmed beam decreases slightly with the increase of f_m, while that of the filmed beam is almost uniform.

3.2 Influence of internal damping on plate vibration characteristics

Figure 6 shows the relationship between the natural frequency and the vibration mode that are explained in the table outside this figure. The shift in the natural frequency for vibration modes makes a comparison between the numerical and experimental modal analyses in reference to the plates having thicknesses h of 2mm and 4mm. In particular, damping coefficient β is varied to study the influence of internal damping on the natural frequency of plate. In the case of the numerical result, indicating a tendency to increase with shifting the vibration mode to high order without reference to varying h and β, the natural frequency changes quantitatively due to varying h and β. However, the changes with respect to β are restrained except for high order of h=4mm. Such changes are caused by β, which is assumed to be, respectively, 10^{-4} when h is 2mm and 4mm. This means that the influence of β has volume effects, because the influence of β occurs to h=4mm more clearly regardless of the assumption of β. On the other hand, although the tendency of the experimental result corresponds with that of the numerical result, the experimental β is much smaller than the above β, being in the vicinity of the range between 10^{-6} and 10^{-8}, as shown in Fig.5. In the case of the numerical result, calculated with the real β, we have already made sure that the influence of β hardly occurred at natural frequencies. Consequently, when h=4mm, the difference between the numerical natural frequency having β=0 and the experimental natural frequency should be not affected by β. The experimental natural frequency is considered to be almost identical to the numerical natural frequency when h=2mm, so that

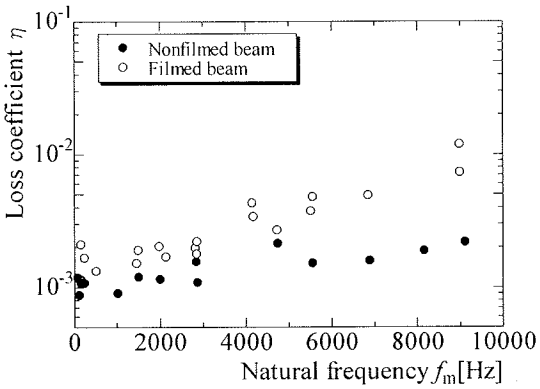

Fig.4 Relationship between loss coefficient and natural frequency

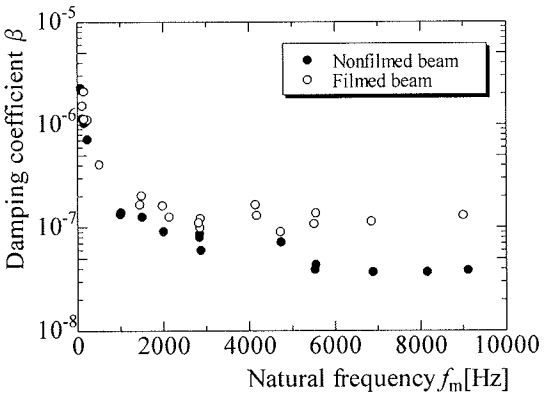

Fig.5 Relationship between damping coefficient and natural frequency

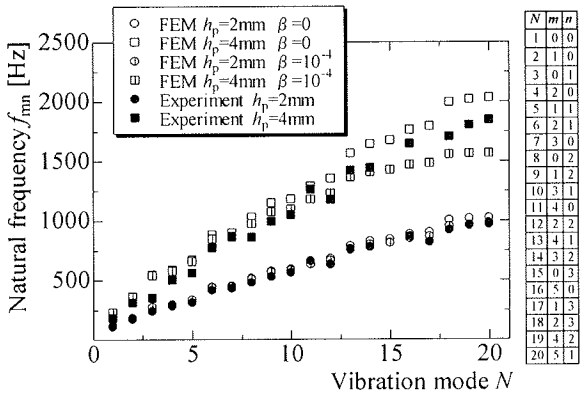

Fig.6 Relationship between natural frequency and vibration mode

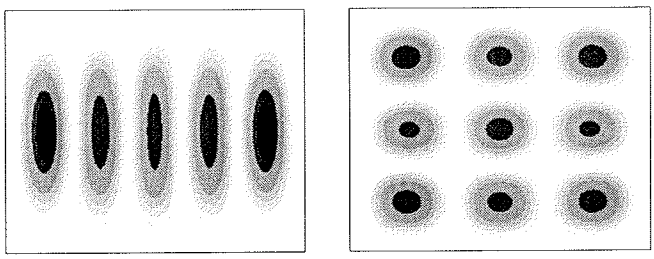

(a) f_e=647Hz (b) f_e=680Hz

Fig.7 Flexural displacement distribution of rectangular plate not having internal damping (β=0)

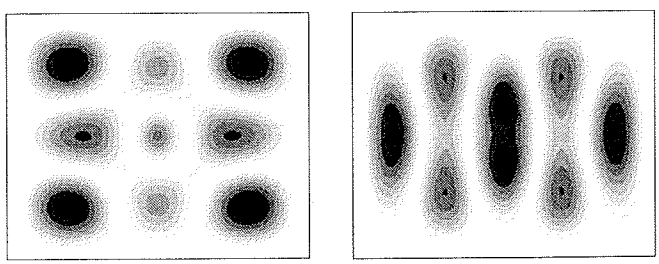

(a) f_e=646Hz (b) f_e=679Hz

Fig.8 Flexural displacement distribution of rectangular plate having internal damping (β=10^{-5})

the support condition is regarded as the major cause of such a difference. Because the four sides of the experimental plate are not clamped so completely as those of the analytical models and plate rigidity is proportional to a plate thickness cubed, the increase in the plate thickness makes the incompletion of the clamped support promoted and the rigidity of the plate structure weakened. Hence, the increase in the plate thickness and the shift in the vibration mode to high order cause the experimental natural frequency to change to a lower frequency.

Figures 7 (a) and (b) show the distributions of the numerical flexural displacement with respect to the plates not having internal damping when the point force is applied to each plate and is set to be 1N; the excitation frequencies are set to be 647Hz and 680Hz, respectively. The distributions represent clearly (4,0) and (2,2) modes, because the natural frequencies f_{40} and f_{22} exist in the proximity of those excitation frequencies f_e. In order to study the influence of internal damping on vibration modes, Figures 8 (a) and (b) show the flexural displacement distribution of the plate having internal damping, which is assumed as $\beta=10^{-5}$. The excitation frequencies are set to be 646Hz and 679Hz, respectively. The distributions represent the (2,2) and (4,0) modes at f_e=646Hz and 679Hz, respectively. Such an appearance of the vibration modes suggests that internal damping concerns those formations.

Figures 9 (a) and (b) show the distribution of the flexural displacement along the x axis with respect to Figs.7 and 8 and experimental results. W_0 is a nondimensional displacement normalized by each maximum flexural displacement and always has a positive value to compare the numerical and experimental results. The influence of internal damping is estimated by the comparison between the experimental distributions of the nonfilmed and filmed plates, so that the above suggestion is proved to a certain extent, because the appearance of the experimental vibration modes is similar to that of the numerical vibration modes. And the numerical modal shapes of the plate vibration make a difference in appearance because of changes in β if those vibration modes are identical.

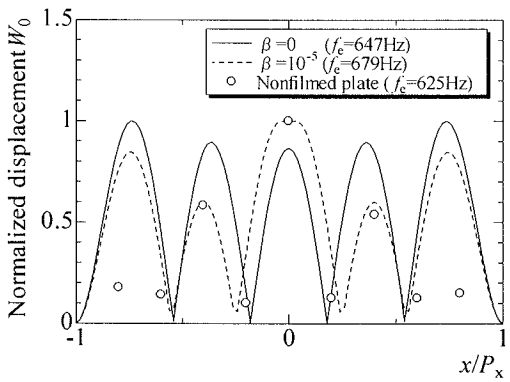

(a) (4,0) mode

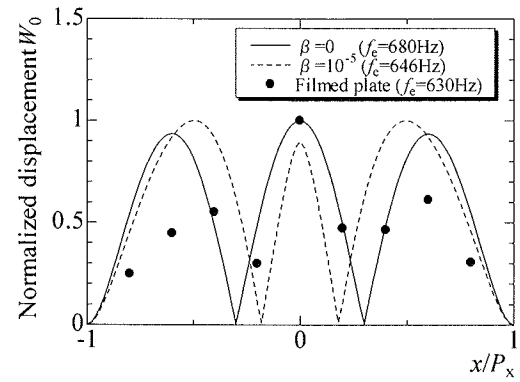

(b) (2,2) mode

Fig.9 Flexural displacement distribution of rectangular plate along x axis

3.3 Influence of internal damping on acoustic radiation

Figure 10 shows the distribution of the sound pressure level on the x-z plane including the origin to understand a rough acoustic radiation from the plate, which has the thickness h of 2mm and the damping coefficient β of 0 and is excited by the point force having excitation frequency f_e=647Hz. The vibration mode becomes (4,0), as shown in Fig.7 (a), so that the distribution of the sound pressure level in the vicinity of the plate surface corresponds to the modal shape of the plate vibration. However, the modal shape of the plate vibration affects the sound field not only in the vicinity of the plate surface but also in far region from its surface within this figure.

In order to evaluate quantitatively the influence of internal damping on the magnitudes of the plate vibration and acoustic radiation, Figure 11 shows the vibration power E_p of the entire plate and the acoustic power E_a passing through the calculating plane, which is at a distance of 50mm from the plate surface and is identical to the plate in area, when h=2mm and β is varied as 0, 10^{-5} and 10^{-4}. The vibration power is found based on the average quadratic velocity, which is calculated by integrating the flexural displacement along the entire surface of the plate. The influence of internal damping is evaluated by the comparison of the vibration power, whereas the excitation frequency is not only at the natural frequency, as described above, but also in a wide frequency range. E_p changes greatly with shifting the excitation frequency and increases extremely at the peak frequencies. Basically determined by natural frequencies of each plate, the peak frequencies are the natural frequencies corresponding to the vibration modes having even orders. Because the point force is applied to the center of the plate, the appearances of odd modes

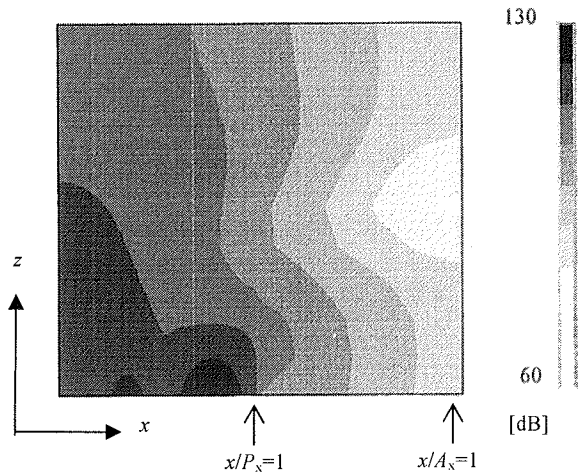

Fig.10 Distribution of sound pressure level on x-z plane (h_p=2mm, β=0, f_e=647Hz)

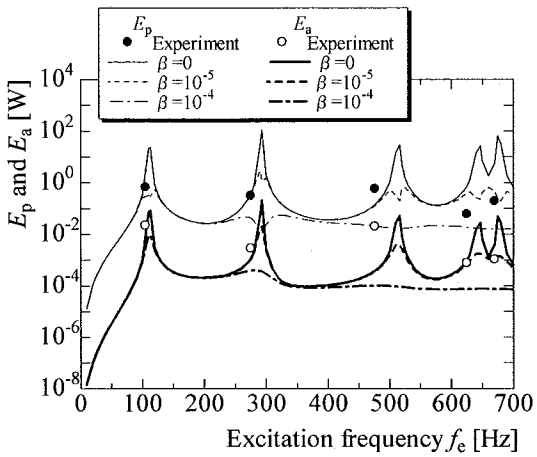

Fig.11 Power of plate vibration and acoustic radiation

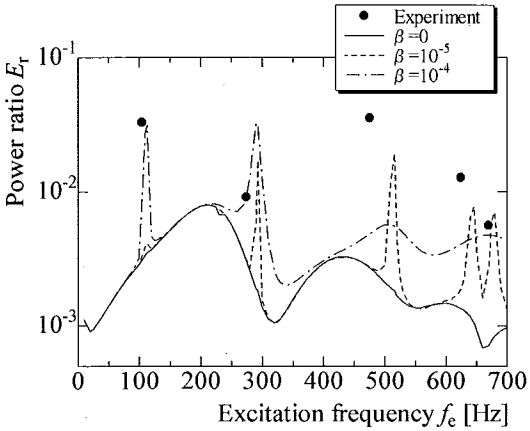

Fig.12 Power ratio of acoustic radiation to plate vibration

are restrained. E_p decreases with the increase of β in the proximity of the peak frequencies and the decrease is promoted by shifting the natural frequency to high orders, so that the peaks of E_p hardly occur at the natural frequencies of high orders when $\beta=10^{-4}$.On the other hand, E_a changes with respect to f_e similarly to E_p, because acoustic radiation characteristics in the vicinity of the plate surface depend greatly on plate vibration characteristics, as described above. In order to verify such a numerical result, experimental results at the natural frequencies, at which (0,0), (2,0), (0,2), (4,0) and (2,2) appear, are indicated in this figure when h=2mm. Although β ranged from 10^{-8} to 10^{-6} in Fig.5, these experimental results are close to the numerical data of $\beta=10^{-5}$ and 10^{-4}. The real β, which is predicted from the comparison between the numerical and experimental results, is greater than β in numerical analysis, including not only internal damping but also damping along the support sides. Thus β should be overestimated in such a FEM analysis. Here, in order to the a quantitative comparison between the magnitudes of the acoustic radiation and plate vibration, the power ratio E_r is defined as the ratio of E_a to E_p.

Figure 12 shows changes in E_r based on E_p and E_a in Figs.11 with respect to f_e, and then experimental E_r is also indicated, calculated using the experimental E_a and E_p in Fig.11. When β=0, E_r changes in the opposite manner to E_p and E_a. Because air on an antinode flows into neighboring nodes with respect to the plate vibration, which is much shorter in wavelength than the radiation sound, the plate vibration cannot efficiently compress the air that is medium of sound. Consequently, E_r decreases in the proximity of the natural frequencies due to restraint of the acoustic radiation. When $\beta=10^{-5}$ and 10^{-4}, there are some cases where E_r increases extremely in the proximity of the natural frequencies. The major cause of such increases is the above changes in E_p when β is varied, while, as explained in Fig.9, the changes in the modal shape of the plate varying β make the above changes in E_a restrained in comparison with those in E_p. On the other hand, being almost identical to the numerical E_r having $\beta=10^{-4}$ at (0,0) mode, the experimental E_r is close to the numerical E_r having $\beta=10^{-5}$ in high orders of the plate vibration. Such a shift in β proves that experimental β decreased with the increase of natural frequency f_m, as shown in Fig.5.

4. Conclusion

For the rectangular plate constructed of aluminum used for members of a lightweight structure, the influence of internal damping on the vibration and acoustic radiation characteristics was investigated by the experiment and FEM analysis. In order to study such an influence, first of all, internal damping of the aluminum is experimentally evaluated using the beam-shaped test specimen as the loss coefficient, and then the beam attaching the polyolefin film to the both surfaces is also used to vary internal-damping characteristics.

The loss coefficient of the aluminum increases slightly with the natural frequency of beam, and the changes in the loss coefficient are promoted by the existence of thin film layer. With respect to the plate vibration characteristics, hardly affecting the natural frequency, internal damping induces changes in the vibration mode and the amplitude of flexural displacement. In particular, the influence on the vibration mode reaches not only its appearance but also its modal shape. Consequently, the acoustic radiation is affected by the changes in the modal shape caused by the internal damping from the point of view of distribution characteristics.

References

(1) N. Nakagawa, Y. Sekiguchi and A. Azuma: Study on Sound Generating Mechanism Using Vibrational Energy and Sound Energy: 1st Report, Effects of Dissipation Energy on Vibrational and Sound Energy Flow, Trans. of JSME, 61-590 (C), (1995), pp.3820-3826. (in Japanese)

(2) N. Nakagawa, Y. Sekiguchi and A. Azuma: Study on Sound Generating Mechanism Using Vibrational Energy and Sound Energy: 2nd Report, Relationship between Structural Intensity Vortex Flow and Sound Field, Trans. of JSME, 62-593 (C), (1996), pp.97-103. (in Japanese)

(3) N. Nakagawa, Y. Sekiguchi. and A. Azuma: Study on Sound Generating Mechanism Using Vibrational Energy and Sound Energy: 3rd Report, Proposal of Energy Transformation Efficiency of Rectangular Plate from Vibration to Sound, Trans. of JSME, 62-604 (C), (1996), pp.4520-4527. (in Japanese)